



Global distribution and climatic controls of natural mountain treelines

Journal:	<i>Global Change Biology</i>
Manuscript ID	GCB-23-1212
Wiley - Manuscript type:	Research Article
Date Submitted by the Author:	30-May-2023
Complete List of Authors:	<p>He, Xinyue; Southern University of Science and Technology, School of Environmental Science and Engineering Jiang, Xin; Southern University of Science and Technology, School of Environmental Science and Engineering Spracklen, Dominick; University of Leeds, School of Earth and Government Holden, Joseph Liang, Eryuan; Institute of Tibetan Plateau Research, Chinese Academy of Sciences, Liu, Hongyan; Peking University, Xu, Chongyang; Hebrew University of Jerusalem Robert H Smith Faculty of Agriculture Food and Environment Du, Jianhui; School of Geographical Science and Planning, Sun Yat-Sen University, Guangzhou 510275, China; Zhu, Kai; University of Michigan, School for Environment and Sustainability Elsen, Paul; Wildlife Conservation Society, Global Conservation Program Zeng, Zhenzhong; Southern University of Science and Technology, School of Environmental Science and Engineering</p>
Keywords:	treeline, forest boundary, climate, mountain ecosystems, alpine area
Abstract:	<p>Mountain treelines are thought to be sensitive to climate change. However, how climate impacts mountain treelines is not yet fully understood as treelines may also be affected by other human activities. Here we focus on “closed-loop” mountain treelines (CLMT) that completely encircle a mountain and are less likely to have been influenced by human land-use change. We detect a total length of ~916,425 km of CLMT across 243 mountain ranges globally and reveal a bimodal latitudinal distribution of treeline elevations with higher treeline elevations occurring at greater distances from the coast. Spatially, we find that temperature is the main climatic driver of treeline elevation in boreal and tropical regions, whereas precipitation drives CLMT position in temperate zones. Temporally, we show that 70% of CLMT have moved upwards, with a mean shift rate of 1.2 m/year over the first decade of the 21st century. CLMT are shifting fastest in the tropics (mean of 3 m/year), but with greater variability. Our work provides a new mountain treeline database that isolates climate impacts from other anthropogenic pressures, and has important implications for biodiversity, natural</p>

	resources, and ecosystem adaptation in a changing climate.

SCHOLARONE™
Manuscripts

Global distribution and climatic controls of natural mountain treelines

Xinyue He^{1,2}, Xin Jiang¹, Dominick V. Spracklen², Joseph Holden³, Eryuan Liang^{4,5},

Hongyan Liu⁶, Chongyang Xu⁶, Jianhui Du⁷, Kai Zhu^{8,9}, Paul R. Elsen¹⁰, Zhenzhong Zeng^{1*}

¹ School of Environmental Science and Engineering, Southern University of Science and Technology, Shenzhen, China

² School of Earth and Environment, University of Leeds, Leeds, UK

³ School of Geography, University of Leeds, Leeds, UK

⁴ Key Laboratory of Alpine Ecology, Institute of Tibetan Plateau Research, Chinese Academy of Sciences, Beijing, China

⁵ CAS Center for Excellence in Tibetan Plateau Earth Sciences, Beijing, China

⁶ College of Urban and Environmental Science and MOE Laboratory for Earth Surface Processes, Peking University, Beijing, China

⁷ School of Geography and Planning, Sun Yat-Sen University, Guangzhou, 510275, China

⁸ Department of Environmental Studies, University of California, Santa Cruz, California, USA

⁹ Institute for Global Change Biology and School for Environment and Sustainability, University of Michigan, Ann Arbor, MI 48109, United States

¹⁰ Wildlife Conservation Society, Global Conservation Program, Bronx, NY, USA

*Correspondence to: zengzz@sustech.edu.cn (Z. Zeng)

Manuscript for *Global Change Biology*

30 May 2023

23 **Abstract**

24 Mountain treelines are thought to be sensitive to climate change. However, how climate impacts
25 mountain treelines is not yet fully understood as treelines may also be affected by other human
26 activities. Here we focus on “closed-loop” mountain treelines (CLMT) that completely encircle
27 a mountain and are less likely to have been influenced by human land-use change. We detect a
28 total length of ~916,425 km of CLMT across 243 mountain ranges globally and reveal a
29 bimodal latitudinal distribution of treeline elevations with higher treeline elevations occurring
30 at greater distances from the coast. Spatially, we find that temperature is the main climatic driver
31 of treeline elevation in boreal and tropical regions, whereas precipitation drives CLMT position
32 in temperate zones. Temporally, we show that 70% of CLMT have moved upwards, with a
33 mean shift rate of 1.2 m/year over the first decade of the 21st century. CLMT are shifting fastest
34 in the tropics (mean of 3 m/year), but with greater variability. Our work provides a new
35 mountain treeline database that isolates climate impacts from other anthropogenic pressures,
36 and has important implications for biodiversity, natural resources, and ecosystem adaptation in
37 a changing climate.

38

39 **Keywords:** treeline, forest boundary, climate, mountain ecosystems, alpine area

40

41 **1. Introduction**

42 The mountain treeline is the upper altitudinal limit of tree growth toward the top of mountains,
43 a transitional zone from forests to treeless alpine vegetation (Körner & Paulsen, 2004). Treeline
44 ecotones play important environmental roles, including as habitats for endemic species and by
45 contributing to water supply (Grace, 1989). Mountain treelines are important indicators of the
46 impact of climate change on upland ecosystems (Verrall & Pickering, 2020; Lu *et al.*, 2021) as
47 they are strongly associated with growing season lengths and minimum daily temperatures
48 (Paulsen & Körner 2014). Consequently, as a response to global warming, mountain treelines
49 are expected to shift upward as high elevations become more favourable for tree establishment
50 under a changing climate (Holtmeier & Broll, 2005; Du *et al.*, 2018). Furthermore, treeline
51 shifts give rise to novel high-elevation vegetation patterns and could redefine habitable area for
52 forest-dependent species in a warmer future world (Bolton *et al.*, 2018; Mohapatra *et al.*, 2019).
53 However, the treelines in many mountain regions have been heavily altered by land-use change
54 and land-use management (Gehrig-Fasel *et al.*, 2007; Ameztegui *et al.*, 2016). Such land-use
55 driven treelines are generally lower than the elevation of the local theoretical climatic treelines,
56 making it difficult to isolate potential influences of climate on treeline position and obscuring
57 the impact of climate change on treeline shifts. Therefore, accurate and reproducible detection
58 of natural mountain treelines and their shifts are of great importance to understanding global
59 climate change and the associated response of vegetation dynamics in alpine areas in natural
60 systems.

61
62 Previous studies reporting local treeline sites have mainly relied on field investigation (Wardle
63 & Coleman, 1992; Liang *et al.*, 2014; Elliott *et al.*, 2015; Sigdel *et al.*, 2018). While such studies
64 have enhanced our understanding of treeline patterns, a key limitation of field-based studies is
65 sparse geographic coverage. Remote sensing can overcome such a limitation by providing
66 globally consistent coverage, but the determination of treeline positions only through visually
67 interpreting satellite imagery (Paulsen & Körner, 2014; Irl *et al.*, 2016; Karger *et al.*, 2019) is
68 time-consuming and labour-intensive at large spatial scales. Recently, regional attempts to
69 combine remote sensing data with automated image processing techniques have emerged (Wei
70 *et al.*, 2020; Xu *et al.*, 2020; Wang *et al.*, 2022; Birre *et al.*, 2023), but inconsistent analytical
71 approaches and treeline definitions complicate regional comparisons and make it difficult to
72 generalize global patterns.. Early assessment at the global scale suggested that low temperatures
73 limited tree growth at treelines (Körner & Paulsen, 2004), but there is also regional evidence
74 that tree growth at the treeline does not increase under global warming due to moisture

75 limitations (Liang et al., 2014; Lyu et al., 2019; Camarero et al., 2021). A generalizable pattern
76 of the climatic limiting factors of global treelines is still lacking.

77

78 The aforementioned challenges and limitations associated with delineating treelines and
79 determining climatic influences on treeline positions have hindered our understanding of the
80 global impact of climate on treelines in natural systems. To address this issue, we focused on
81 “closed-loop” mountain treelines (CLMT)—treelines with a continuous band of tree cover
82 around a mountain. Such systems are less likely to have been influenced by land-use change.
83 By focusing on this subset of treelines, we are better able to exclude treelines that may be
84 impacted by topographic constraints or anthropogenic land use in order to isolate the effects of
85 climate on mountain treelines in natural systems. An advance over previous studies that only
86 provide a handful of data points for each treeline is a complete depiction of treeline at 30 m
87 resolution. Our approach allows us to calculate the treeline elevation around the entire treeline,
88 providing unprecedented detail on the variability of treeline elevation at the local scale. More
89 importantly, using CLMT as a proxy for natural treelines with little influence from land-use
90 change allows us to make a new and more robust assessment of how natural treelines are
91 responding to changes in climate.

92

93 Here, we map closed-loop treelines in mountain regions globally in 2000 based on remote
94 sensing, via integrating a high-resolution tree cover map (Hansen *et al.*, 2013) with a digital
95 elevation model at the same spatial resolution (Tachikawa *et al.*, 2011). For this purpose, we
96 develop a novel automatic detection algorithm that can produce consistent characterizations of
97 CLMT across space. Our detection of mountain treeline is based on tree cover data that consider
98 trees as any vegetation taller than 5 m (Hansen *et al.*, 2013), using a 5% tree cover threshold to
99 delineate forested and non-forested areas. The algorithm starts from the highest elevation point
100 for each mountain range and generates a forest boundary map from which we extract the closed-
101 loop treelines. To further ensure that our CLMT are natural treelines that are not impacted by
102 anthropogenic disturbances, we conduct a manual inspection of high-resolution imagery to
103 remove treelines with any indication of anthropogenic land use and restrict our analysis to
104 regions where the human footprint is low (Mu et al., 2022). To understand which bioclimatic
105 factors control the position of natural mountain treelines from global to local scales, we use the
106 gradient boosting decision trees (GBDT) model (Friedman, 2001) to calculate the feature
107 importance of each temperature or precipitation variable. Further, we map the new natural

108 treeline positions in 2010 using the same algorithm above and the amount of tree cover in 2010
109 (Hansen *et al.*, 2013) to explore the shifting of mountain treelines in natural systems.

110

111 **2. Methods**

112 **2.1. Tree canopy cover data**

113 We used a high-resolution remote sensing global map of tree canopy cover for the year 2000
114 (available at https://earthenginepartners.appspot.com/science-2013-global-forest/download_v1.7.html;
115 Hansen *et al.*, 2013) to delineate forested and non-forested areas.

116 The dataset was produced at a 30 m resolution based on multiple types of forest sample data
117 and spectral curves of Landsat time series using a decision tree method (Hansen *et al.*, 2013).

118 To test which tree cover threshold is suitable for treeline mapping, we undertook a sensitivity
119 analysis with different thresholds in mountains, finding there is little difference among different
120 thresholds from 0 to 10% (examples refer to Figs. S1–S3). Thus, we took the mean value of 0
121 to 10%, namely 5%, as the tree cover threshold, and define the treeline to be the transition zone
122 above which tree cover is $\leq 5\%$ and below which tree cover is $> 5\%$. We then binary-classified
123 the tree canopy cover data using the threshold, assigning a value of 1 for the alpine land zone
124 (the area above treeline) with tree cover $\leq 5\%$ (non-forested area), and 0 for pixels with greater
125 than 5% tree cover (forested area).

126

127 **2.2. Topography data**

128 We combined global mountain polygons with a high-resolution digital elevation model to
129 restrict the search area of mountain treelines. Mountain boundaries were collected from the
130 Global Mountain Biodiversity Assessment (GMBA) inventory (version 1.2; available at
131 https://ilias.unibe.ch/goto_ilias3_unibe_cat_1000515.html;
132 Körner *et al.*, 2017). The GMBA
133 inventory delineated global mountains into discrete regions (polygons) based on topographic
134 ruggedness metrics and expert delineation (Körner *et al.*, 2017). The elevation information in
135 mountains was provided by the Advanced Spaceborne Thermal Emission and Reflection
136 Radiometer Global Digital Elevation Model (version 3; available at <https://earthdata.nasa.gov/>;
Tachikawa *et al.*, 2011) at a spatial resolution of 30 m.

137

138 **2.3. Iterative mountain treeline extraction algorithm**

139 We developed an algorithm to automatically detect CLMT (Fig. S4). We first determined the
140 coordinates of the highest peak within each mountain region. The algorithm starts at this peak
141 point if it is within the alpine area that is non-forested, then expands outward (i.e., downslope),

142 and determines all other pixels of the image that are connected to the point and equivalent
143 (marked as “1”). The eight neighbourhood region of the pixel $I(x,y)$ is expressed as:

$$144 \quad R8 = \{(x+i, y+j) ; i, j \in (-1, 1)\} \quad (1)$$

145 where I, j are integers. In the collection of the eight neighbourhood pixels, if $I(x,y) = I(x+i,y+j)$,
146 there are connected relationships. The connected domain generated by this method is the
147 connected alpine area. Because the algorithm determines the starting search point, we marked
148 only one connected domain (namely the treeline zone) after one iteration.

149

150 To accelerate the efficiency of the algorithm, we set search blocks to determine the full
151 altitudinal range of treelines within mountain ranges (Fig. S4). Specifically, the first round of
152 the search takes the highest point of the mountain as the centre and the buffer zone with a side
153 length of R as the search area for the treeline. After testing, the square area with 8,000
154 rows/ranks (side length R about 240 km) covered most alpine areas of mountains. For some of
155 the mountaintops larger than this range, we expanded the side length to ~ 720 km to ensure that
156 all close-loop mountain treelines of the world’s mountaintops were covered.

157

158 There may be multiple treelines within a mountain range because a mountain may have multiple
159 peaks. To account for this, we next searched for the second highest starting point (i.e., the
160 highest point of the unsearched part) and repeated the process until the selected highest point
161 was covered by forests (tree cover $>5\%$).

162

163 After each iteration, the loops that were determined to be “open” were removed. Focusing only
164 on closed treeline loops generated from the algorithm, we then visually inspected all loops using
165 Google Earth (with spatial resolution ranging from 15 m to ~ 15 cm) to further exclude treelines
166 with apparent signs of anthropogenic disturbances, such as roads, buildings, or croplands and
167 removed the part of water bodies (i.e., pixels that were determined to be water). Last, we filled
168 all the holes in the closed-loop polygons using the “imfill” function and extracted the edges of
169 the binary images using the “bwperim” function in Matlab R2019a to obtain the CLMT
170 positions.

171

172 To validate the robustness of the elevational distribution of CLMT derived from satellite images,
173 at the pixel level, we used an independent validation dataset by manual interpretation using
174 Google Earth’s high-resolution images. We randomly produced 100 validation samples at a
175 spatial resolution of 30 m. On a larger scale, we validated our CLMT database by comparison

176 with *in situ* measures ($n = 62$; Table S1). For each treeline site, we corresponded it to the closest
177 treeline loop detected in this study and compared its elevation with the range of the
178 corresponding treeline loop.

179

180 **2.4. Climate data**

181 Considering the effect of climatic lag effects on treelines (Harsch *et al.*, 2009), we used the
182 climate data from WorldClim (version 2.1; <https://www.worldclim.org/data/worldclim21.html>;
183 Fick and Hijmans, 2017), which provided the average for the years 1970–2000 at a resolution
184 of 30 seconds ($\sim 1 \text{ km}^2$), to understand which climate variables are important in controlling
185 treeline elevations. We used bioclimatic variables, which were derived from monthly
186 temperature and precipitation. A total of eight temperature variables and eight precipitation
187 variables were included, representing annual trends, seasonality, and extreme or limiting
188 environmental factors. They are annual mean temperature (annual T), temperature seasonality
189 (T seasonality; calculated as the standard deviation of the monthly mean temperatures, then
190 multiply by 100), the maximum temperature of the warmest month (maximum T), the minimum
191 temperature of the coldest month (minimum T), mean temperature of the wettest quarter (wet
192 season T), mean temperature of the driest quarter (dry season T), mean temperature of the
193 warmest quarter (warm season T), mean temperature of the coldest quarter (cold season T),
194 annual precipitation (annual P), precipitation of the wettest month (maximum P), precipitation
195 of the driest month (minimum P), precipitation seasonality (P seasonality; calculated as the
196 coefficient of variation, which is the ratio of the standard deviation to the mean), precipitation
197 of the wettest quarter (wet season P), precipitation of the driest quarter (dry season P),
198 precipitation of the warmest quarter (warm season P), and precipitation of the coldest quarter
199 (cold season P). A ‘quarter’ here refers to any consecutive three months. For example, the
200 coldest quarter consists of the three months that are colder than any other set of three
201 consecutive months. For each pixel determined to be on a CLMT, we extracted the values of all
202 16 climate variables.

203

204 **2.5. Gradient boosting decision trees (GBDT) model**

205 We applied a GBDT method to model the treeline elevation as a function of climate factors.
206 The GBDT model is a type of tree model with good interpretability for feature values
207 (Friedman, 2001), which assembles and iterates over multiple regression trees, with the values
208 of the negative gradient of the loss function in the model as an approximation of the residuals
209 of the lifting tree algorithm in the regression problem (Ke *et al.*, 2017). It is flexible in handling

210 large amounts of data and often performs well in dealing with complex relationships in data
211 (Ke *et al.*, 2017). The GBDT initializes a weak learner, estimating a constant value of the loss
212 of function minimization, and then creates decision trees according to the datasets and performs
213 iterative training on them. Next, it calculates the negative gradient for loss of function (residuals)
214 corresponding to each tree, fits a regression tree to the residuals to obtain the leaf node region
215 of the *m*-th tree, and minimizes loss of function by estimating the values of all leaf node regions
216 using a linear search. Last, GBDT repeats the above steps until the target evaluation indicator
217 is optimal. Using this model, we calculated the feature importance of each variable and
218 determined the dependent correlations for each factor after the model was built. The GBDT
219 analysis was undertaken in Python 3.7 with the “sklearn.ensemble” module.

220

221 We carried out the GBDT analyses at global and local scales, as well as separately for different
222 climatic belts (i.e., boreal, temperate, and tropical regions). At the global scale, we considered
223 each treeline loop as a sample, namely, mean elevation in a loop of the treeline was the
224 dependent variable and the average of climate variables in a loop were the independent
225 variables. A total of 1,690 samples (treeline loops) were used for the global model. At the local
226 scale, we regarded one treeline pixel as a sample. Hence, in each treeline loop, the repeated
227 GBDT model represents the local effect of climate factors on treeline positions.

228

229 **2.6. Mountain treeline shift rate**

230 We mapped the new treeline positions in 2010 based on the global 2010 tree cover data
231 (available at https://glad.umd.edu/Potapov/TCC_2010/; Hansen *et al.*, 2013; Potapov *et al.*,
232 2015), which is an update of the 2000 tree cover product. Using this dataset, we re-ran the
233 algorithm around treelines to detect the new closed-loop treelines in 2010. Starting from the
234 highest elevation point we detected before, we expanded the rectangular area of the original
235 treeline around by 10 km as the search area. Then we manually checked the results from the
236 1,690 treeline loops to (i) exclude treelines without closed loops; (ii) isolate examples of
237 “broken treeline loops” and restrict them to corresponding areas in 2000 and 2010 (Fig. S5);
238 and (iii) remove outliers (>95th percentile of both increasing and decreasing rates) to avoid the
239 inclusion of any special cases with extremely steep changes. This filtering resulted in 1,110
240 treeline loops in 2010 (65.7% of all treelines initially assessed) being available for analysis of
241 the treeline change. The main reason for the reduction in number of treeline loops between 2000
242 and 2010 is that some of the closed-loop treelines detected in 2000 did not form closed loops in
243 2010. We then calculated the mean elevation of closed-loop treelines in 2010 and the

244 corresponding treelines in 2000 and used the difference to represent the treeline change over
245 the 10-year period. The treeline shift rate (m/year) at each treeline loop was calculated as
246 follows:

$$247 \quad \text{Shift rate} = \frac{\text{mean elevation 2010} - \text{mean elevation 2000}}{10 \text{ yrs}} \quad (2)$$

248

249 **3. Results**

250 **3.1. A map of global closed-loop mountain treelines**

251 We detected 27,468,662 closed-loop mountain treeline positions (pixels at 30 m resolution)
252 across 243 mountain ranges globally. The total length of the closed-loop treelines we detected
253 is ~916,425 km. Those treeline pixels form 1,690 treeline loops covering all continents except
254 Antarctica, ranging from 64°N (Khrebet Polyarnyy, Russia) to 46°S (Princess Mountains, New
255 Zealand), with mean elevations spanning from 489 ±283 m on Khrebet Chayatyn (Russia) to
256 4,528 ±104 m on Ruwenzori (Uganda, Kenya). The average length of these closed-loop
257 treelines is 542 km, and the average alpine land area above them is 142 km². To visualize global
258 patterns of the elevation of CLMT, we calculated the mean elevation for each treeline loop and
259 plotted their locations using the mean latitude and longitude of treeline pixels at 30 m resolution
260 in each loop (Fig. 1a). The CLMT derived from satellite tree cover data are consistent with fine
261 resolution remote sensing images available on Google Earth (Fig. 1b–g). At the pixel level, the
262 CLMT showed good agreement with manually interpreted data at 30 m resolution ($R^2 = 0.96$;
263 Fig. S6). On a larger scale, the validity of our CLMT database was further supported by
264 corroboration against *in situ* measures from previous studies ($n = 62$ measurements; Table S1),
265 which fall within the elevation range of CLMT loops ($R^2 = 0.98$; Fig. S7).

266

267 We found a bimodal pattern for the closed-loop mountain treeline elevation along latitude, with
268 peaks at the equator and ~25°N (Fig. 2a). Between 0° and 10°, the elevation of CLMT is
269 symmetrical in the northern and southern hemispheres, but beyond this range, treeline
270 elevations in the northern hemisphere are higher than those in the southern hemisphere at
271 equivalent latitudes (Fig. 2a), which is attributed to the oceanic influence on a smaller southern
272 landmass (Testolin *et al.*, 2020). Our global CLMT distribution is consistent with previous
273 global assessments, though there are some differences. In the tropics, the elevation of CLMT
274 reaches up to 3,500 m (Fig. 2), a lower elevation than in a recent global assessment by Testolin
275 *et al.* (2020) that reported tropical treelines higher than 4000 m. This discrepancy may be due
276 to our strict definition of trees, >5 m height, as well as the exclusion of some unilateral and non-

277 closed treelines in high mountains. At low latitude (especially at 0-20°N), there is large
278 variation in the range of CLMT elevation (Fig. 2a). Among different continents, South America
279 has a large CLMT elevation range variation. At 50°N–60°N and 20°N–30°N, many mountains
280 in Asia and North America have similar treeline elevations, whereas there is a rather different
281 behaviour at 30°N–50°N where treelines in North America are higher than those in Europe and
282 Asia (Fig. 2a). To help understand what causes this behaviour, we calculated the distance to the
283 coast for each treeline. We found lower treelines in coastal mountains at the same latitude (Fig.
284 2a) as has been suggested in the literature (Irl *et al.*, 2016), which can be largely attributed to
285 the thermo-dynamic effect of large high-elevation landmasses (Karger *et al.*, 2019). At 340°N–
286 60°N, mountains close to the coast have lower treelines than their latitude might suggest (i.e.,
287 fall below the fitted curve; Fig. 2a). Similarly, along with longitude decreasing from 150°W to
288 100°W, treeline elevations in North America increase due to an increase in the distance to the
289 coast (Fig. 2b).

290

291 **3.2. Climatic determinants of closed-loop mountain treelines**

292 We found that T seasonality, cold season P, and warm season T predict nearly 60% of the spatial
293 distribution of CLMT globally (Fig. 3a). We then assessed how the three leading factors
294 modulated the elevation of CLMT spatially. The results showed the abrupt transition of CLMT
295 elevation occurring at the T seasonality threshold of ~9°C, but attenuated transitions in areas
296 where T seasonality exceeded 10°C (Fig. S8a). Similarly, there is a CLMT elevation gradient
297 that is spatially driven by cold season P, with abrupt transitions occurring at the thresholds of
298 320 mm and 450 mm along the gradient of cold season P (Fig. S8b). By contrast, we did not
299 find such a dramatic transition of CLMT elevation along the warm season T gradient (Fig. S8c).

300

301 Collectively, temperature-related factors (64%) are more important than precipitation-related
302 factors for limiting CLMT elevations on a global scale (Fig. 3a). In different latitudinal belts,
303 temperature-related factors are most important in boreal and tropical regions, especially the
304 temperature of the warmest and the wettest quarters, respectively, while precipitation dominates
305 the CLMT elevation in temperate regions (Fig. 3b–d). Our results confirm the importance of
306 temperature during the warm part of the year in the boreal zone (Jobbágy & Jackson, 2000), but
307 suggest that precipitation is more important than temperature in temperate regions. It agrees
308 with climatic sensitivity of tree growth in the Northern Hemisphere (Gao *et al.*, 2022). Especially
309 under dry environmental conditions, moisture availability is crucial to limiting tree growth in
310 the treeline ecotone (Liang *et al.*, 2014; Ren *et al.*, 2018).

311
312 Our study provides vastly more data points for each treeline compared to previous global
313 assessments (Jobbágy & Jackson, 2000; Körner & Paulsen, 2004), allowing us to explore for
314 the first time what controls treeline position at a local scale. We found that temperature remains
315 the dominant explanation for the altitudinal variation of 76% of the treeline within a single
316 treeline loop with similar climatic conditions (Fig. S9).

317

318 **3.3. Shifts in closed-loop mountain treelines**

319 Between 2000 and 2010, mountain treelines have shifted upwards at 777 out of the 1,110
320 treeline loops (70%) and downward at 333 treeline loops (Fig. 4a). The mean global treeline
321 shift rate was an upward shift of 1.2 m/year, which is consistent with case studies of treeline
322 change, with rates >1 m/year reported in the literature (Table S2). A synthesis of treeline shift
323 rates reported in the literature suggests the rate was 0.67 m/year before 1970 compared to 4.36
324 m/year after 1970 and 6.16 m/year after 2000 (Fig. S10; Table S2). This provides evidence that
325 the rate of change in treeline elevation is accelerating, possibly due to recent rapid climate
326 change (Bolton *et al.*, 2018). Treeline shift rates in the tropics (mean of 3.1 m/year) were higher
327 than those in boreal and temperate regions (Fig. 4b). The faster changes in the tropics could be
328 related to hydrothermal conditions: in the tropics, higher temperature and more abundant
329 precipitation bring a longer growing season, which naturally favours the growth of seedlings
330 and young trees. By contrast, there is a slight downward shift in temperate regions (an average
331 of -0.5 m/year), where the position of the treeline is dominated by precipitation (Fig. 3c). This
332 could be due to decreasing precipitation in some mountain areas of the temperate zone, for
333 example in northern China (Piao *et al.*, 2010).

334

335 Although the tropical CLMT have the fastest shift rates, their variability is the largest, ranging
336 from -10.2 to 16.9 m/year (Fig. 4b). In the tropics, treeline shift rates greater than 10 m/year in
337 the mountains of Malawi, Papua New Guinea, and Indonesia may reflect a more extreme trend
338 in these tropical systems. In other regions, there are also some treelines that have shifted much
339 more than expected (>10 m/year; Fig. 4b): in boreal regions, these expectations are mainly in
340 Russia and Canada; in temperate regions, they are geographically concentrated in East Asia
341 (North Korea, Japan, and China). On the contrary, there are also cases of treelines receding at
342 a high rate, possibly driven by fire in some areas, either through the physical destruction of trees
343 that acts to lower the existing treelines, or through the destruction of seedlings established
344 upslope that acts to prevent treeline advances (Kim & Lee, 2015). For example, treelines have

345 significantly receded in the western USA where climate and vegetation are favourable for fire
346 (Seven Devils Mountains, Swan Range, etc.; Fig. 4a).

347

348 In addition, independent analysis for the changes in annual maximum Normalized Difference
349 Vegetation Index (NDVI) at CLMT that we identified for the year 2000 shows the NDVI has
350 significantly increased by 3.3% by 2020, at a rate of 0.0012 per year ($P < 0.01$; Fig. S11a).
351 There are significant positive trends in NDVI at treeline zones in boreal, temperate, and tropical
352 regions during 2000-2020 ($P < 0.01$), and tropical areas have the highest rate, approaching
353 0.0016 per year (Fig. S11b). The increase in NDVI occurred at most treeline zones (~90%; Fig.
354 S11c). This greening at the treeline may also be conducive to upward movement of the treeline
355 in the future.

356

357 **4. Discussion**

358 **4.1. Comparison of treeline datasets before and after considering human footprint**

359 Although we have examined CLMT by manual interpretation to remove anthropogenic
360 treelines, we further conduct a stricter assessment of human pressures to check whether our
361 results would still be impacted by human activity. We used a global Human Footprint dataset
362 (Mu et al., 2022) and found 83% of our CLMT in wilderness (Human Footprint < 1) or in highly
363 intact areas (Human Footprint < 4). We then removed those treelines with human footprint
364 values ≥ 4 , re-ran the analysis with the higher human footprint values excluded, and updated all
365 the results above (Figs. S12-14). By comparing these new results with those using the whole
366 dataset, we found a similar pattern along latitude and longitude gradients (Figs. 2 and S12). The
367 results regarding climate dominants (Figs. 3 and S13) and treeline shift rates (Figs. 4b and S14)
368 were also consistent using either approach. Thus, the additional criterion to further focus our
369 analysis on treelines with no human disturbance does not alter our overall results or conclusions,
370 and further confirms that our CLMT product can well represent the change and pattern of
371 climatic treelines.

372

373 **4.2. Implications of treeline shifts for carbon, biodiversity, and hydrology**

374 Changing treeline position can affect the carbon cycle, biodiversity, and hydrological processes
375 in mountain environments. Mountain treelines moving upward to higher elevations increase
376 woody biomass at and above the treeline, accumulating carbon and increasing their ability to
377 act as carbon sinks (Lopatin *et al.*, 2006; Tarnocai *et al.*, 2009). However, such increases may
378 be offset by increases in soil respiration, leading to a net loss of ecosystem carbon (Wilmking

379 *et al.*, 2006; Hartley *et al.*, 2012). The ascent of mountain treelines also substantially influences
380 biodiversity patterns at high elevations, with enhanced habitat loss of endemic alpine species
381 within a narrow range of mountains (Wang *et al.*, 2022) and potential expansion of habitat for
382 forest-dependent species whose upper range limits coincide with the treeline ecotones (Elsen *et*
383 *al.*, 2017). For alpine species isolated at the top of mountains, upward treeline shifts could
384 increase the risk of extinction, where there is not enough room for the alpine zone to move
385 upward under future climate change (Dirnböck *et al.*, 2011). In Siberia, for example, we show
386 many treelines have shifted upwards (Fig. 4b), inevitably reducing the area of the tundra, which
387 is rich in floristic and species diversity and supports indigenous land use types. The expansion
388 of Siberian forests has been predicted to continue, thus causing huge losses of tundra in the
389 future (Kruse & Herzsuh, 2022). While we focused here on treeline shifts in areas with
390 minimal human impacts, treeline ascent in areas with pronounced human disturbance will
391 further hinder species' ability to track vegetation changes and likely lead to more pronounced
392 population declines (Feeley & Silman, 2010; Elsen *et al.*, 2020). There are many instances with
393 high high-elevation pressure especially from burning, grazing, and wood harvesting (Bader *et*
394 *al.*, 2008; Jiménez-García *et al.*, 2021). The combined impact of shifting treelines and human
395 disturbances may also affect local livelihoods and act as a double-whammy for sensitive alpine
396 species. In addition, tree expansions into the formerly treeless area may alter downstream water
397 supply. Recent advances of the treeline have decreased the area of alpine tundra, thereby
398 affecting its critical role as a reservoir of freshwater resources and in water release (Barredo *et*
399 *al.*, 2020).

400

401 **4.3. Uncertainties and caveats**

402 To isolate the impacts of climate on treelines, our analysis identifies CLMT that completely
403 encircle a mountain. However, focusing on this kind of treelines could omit some climate-
404 related treelines as climatic treelines may not be in a closed loop shape in some cases. We
405 acknowledge that our CLMT database does not include all climatic treelines, but is a subset of
406 climatic treelines that specifically form a closed loop, because these enable us to analyse
407 climatic determinants with greater confidence. We also note that tree cover can increase in
408 various ways, either through new or existing trees growing above the 5 m height threshold, or
409 existing trees having increased canopy cover. However, our analysis is based on the definition
410 of treeline according to remotely sensed tree cover, and we used this definition to assess treeline
411 position at two time periods and assess change. While our analysis period is short and errors
412 will exist at a pixel scale, our global detection of a shifting treeline provides an early indication

413 of climate-induced changes that need to be carefully monitored in the future. To reduce
414 uncertainties and further advance our understanding of treeline dynamics, future studies require
415 more high-resolution remote sensing products for a longer period and more field data in alpine
416 treeline zones for cross-validation.

417

418 **5. Conclusion**

419 Our study develops a novel remote sensing-based algorithm to map closed-loop treelines across
420 global mountain regions, isolating the effects of climate on treeline position. Our approach
421 provides a globally consistent way of detecting and monitoring closed-loop treelines around
422 mountains, which are more likely to reflect natural systems with minimal impact of land-use
423 change. Focusing on these closed-loop treelines as a proxy for natural treelines allows us to
424 isolate the impacts of climate and climate change on the elevation distribution and change of
425 treelines. We found temperature was the dominant control on natural treelines both at a global
426 and local scale. Our results indicated an upward migration of treelines over the period 2000 to
427 2010 in boreal and tropical regions but a slight downward shift in temperate zones. Our new
428 findings and the global closed-loop mountain treeline database produced in this study also
429 provides a useful tool for biodiversity and carbon assessments, ecological modelling, and
430 analyses of adaptation of species to future climate change.

431

432 **Data availability statement**

433 The data that support the findings of this study are available upon reasonable request from the
434 authors. The global closed-loop mountain treeline database developed in this study can be
435 accessed through <https://hexinyue33.users.earthengine.app/view/clmt>.

436

437 **Acknowledgments**

438 X.H. was funded by a PhD scholarship from Southern University of Science and Technology
439 hosted jointly with the University of Leeds. Z.Z was supported by the National Natural Science
440 Foundation of China (no. 42071022) and the start-up fund provided by Southern University of
441 Science and Technology (no. 29/Y01296122). We thank Hansen/UMD/Google/USGS/NASA
442 for providing the high-resolution tree cover data; NASA and Japan's Ministry of Economy,
443 Trade and Industry for providing the elevation data; Körner for providing the GMBA inventory;
444 Fick and Hijmans for providing WorldClim data; and Google Earth for providing very-high-
445 resolution satellite imagery.

446

447 **Author contributions**

448 X.H., Z.Z., D.V.S. and J.H. designed the research; X.H. performed the analysis and wrote the
449 draft; X.J. helped to code the algorithm; and all the authors contributed to the interpretation of
450 the results and the writing of the paper.

451

452 **References**

- 453 Ameztegui, A., Coll, L., Brotons, L., & Ninot, J.M., 2016. Land-use legacies rather than climate
454 change are driving the recent upward shift of the mountain tree line in the P
455 yrenees. *Global Ecology and Biogeography*, 25(3), pp.263-273.
- 456 Bader, M.Y., Rietkerk, M., & Bregt, A.K. (2008). A simple spatial model exploring positive
457 feedbacks at tropical alpine treelines. *Arctic, Antarctic, and Alpine Research*, 40(2), 269-
458 278.
- 459 Barredo, J. I., Mauri, A., & Caudullo, G. (2020). Alpine tundra contraction under future
460 warming scenarios in Europe. *Atmosphere*, 11(7), 698.
- 461 Birre, D., Feuillet, T., Lagalis, R., Milian, J., Alexandre, F., Sheeren, D., Serrano-Notivoli, R.,
462 Vignal, M., & Bader, M.Y., (2023). A new method for quantifying treeline-ecotone change
463 based on multiple spatial pattern dimensions. *Landscape Ecology*, 1-18.
- 464 Bolton, D.K., Coops, N.C., Hermosilla, T., Wulder, M.A., & White, J.C. (2018). Evidence of
465 vegetation greening at alpine treeline ecotones: three decades of Landsat spectral trends
466 informed by lidar-derived vertical structure. *Environmental Research Letters*, 13(8),
467 084022.
- 468 Camarero, J.J., Gazol, A., Sánchez-Salguero, R., Fajardo, A., McIntire E J B, Gutiérrez E,
469 Batllori E, Boudreau S, Carrer M, Diez J, Dufour-Tremblay G, Gaire NP, Hofgaard A,
470 Jomelli V, Kirilyanov AV, Lévesque E, Liang E, Linares JC, Mathisen IE, Moiseev PA,
471 Sangüesa-Barreda G, Shrestha KB, Toivonen JM, Tutubalina OV, & Wilmking M. (2021).
472 Global fading of the temperature-growth coupling at alpine and polar treelines. *Global*
473 *Change Biology*, 27(9), 1879-1889.
- 474 Dirnböck, T., Essl, F., & Rabitsch, W. (2011). Disproportional risk for habitat loss of
475 high-altitude endemic species under climate change. *Global Change Biology*, 17(2), 990-
476 996.
- 477 Du, H., Liu, J., Li, M.-H., Büntgen, U., Yang, Y., Wang, L., Wu, Z., & He, H.S. (2018).
478 Warming-induced upward migration of the alpine treeline in the Changbai Mountains,
479 northeast China. *Global Change Biology*, 24(3), 1256-1266.
- 480 Elliott, G.P., & Cowell, C.M. (2015). Slope aspect mediates fine-scale tree establishment
481 patterns at upper treeline during wet and dry periods of the 20th century. *Arctic, Antarctic,*
482 *and Alpine Research*, 47(4), 681-692.
- 483 Elsen, P. R., Tingley, M. W., Kalyanaraman, R., Ramesh, K., & Wilcove, D. S. (2017). The
484 role of competition, ecotones, and temperature in the elevational distribution of Himalayan
485 birds. *Ecology*, 98(2), 337-348.

- 486 Elsen, P. R., Monahan, W. B., & Merenlender, A. M. (2020). Topography and human pressure
487 in mountain ranges alter expected species responses to climate change. *Nature*
488 *communications*, 11(1), 1-10.
- 489 Feeley, K. J., & Silman, M. R. (2010). Land-use and climate change effects on population size
490 and extinction risk of Andean plants. *Global Change Biology*, 16(12), 3215-3222.
- 491 Fick, S.E., & Hijmans, R.J. (2017). WorldClim 2: new 1-km spatial resolution climate surfaces
492 for global land areas. *International Journal of Climatology*, 37(12), 4302-4315.
- 493 Friedman, J.H. (2001). Greedy function approximation: a gradient boosting machine. *Annals of*
494 *Statistics*, 29, 1189-1232.
- 495 Gao, S., Liang, E., Liu, R., Babst, F., Camarero, J.J., Fu, Y.H., Piao, S., Rossi, S., Shen, M.,
496 Wang, T., & Peñuelas, J. (2022). An earlier start of the thermal growing season enhances
497 tree growth in cold humid areas but not in dry areas. *Nature Ecology & Evolution*, 6(4),
498 397-404.
- 499 Gehrig-Fasel, J., Guisan, A., & Zimmermann, N.E. (2007). Tree line shifts in the Swiss Alps:
500 Climate change or land abandonment? *Journal of Vegetation Science*, 18, 571-582.
- 501 Grace, J. (1989). Tree lines. *Philosophical Transactions of the Royal Society of London. B,*
502 *Biological Sciences*, 324(1223), 233-245.
- 503 Hansen, M.C., Potapov, P.V., Moore, R., Hancher, M., Turubanova, S.A., Tyukavina, A., Thau,
504 D., Stehman, S.V., Goetz, S.J., & Loveland, T.R. (2013). High-resolution global maps of
505 21st-century forest cover change. *Science*, 342(6160), 850-853.
- 506 Harsch, M. A., Hulme, P. E., McGlone, M. S., & Duncan, R. P. (2009). Are treelines advancing?
507 A global meta-analysis of treeline response to climate warming. *Ecology letters*, 12(10),
508 1040-1049.
- 509 Hartley, I.P., Garnett, M.H., Sommerkorn, M., Hopkins, D.W., Fletcher, B.J., Sloan, V. L.,
510 Phoenix, G.K., & Wookey, P.A. (2012). A potential loss of carbon associated with greater
511 plant growth in the European Arctic. *Nature Climate Change*, 2(12), 875-879.
- 512 Holtmeier, F. & Broll, G. (2005). Sensitivity and response of northern hemisphere altitudinal
513 and polar treelines to environmental change at landscape and local scales. *Global Ecology*
514 *Biogeography*, 14(5), 395-410.
- 515 Hope, G. (2009). Environmental change and fire in the Owen Stanley Ranges, Papua New
516 Guinea. *Quaternary Science Reviews*, 28, 2261-2276.
- 517 Irl, S.D., Anthelme, F., Harter, D.E., Jentsch, A., Lotter, E., Steinbauer, M.J., & Beierkuhnlein,
518 C. (2016). Patterns of island treeline elevation—a global perspective. *Ecography*, 39(5),
519 427-436.

- 520 Jiménez-García, D., Li, X., Lira-Noriega, A., & Peterson, A.T. (2021). Upward shifts in
521 elevational limits of forest and grassland for Mexican volcanoes over three decades.
522 *Biotropica*, 53, 798-807.
- 523 Jobbágy, E.G. & Jackson, R.B. (2000). Global controls of forest line elevation in the northern
524 and southern hemispheres. *Global Ecology Biogeography*, 9(3), 253-268.
- 525 Karger, D.N., Kessler, M., Conrad, O., Weigelt, P., Kreft, H., König, C., & Zimmermann, N.E.
526 (2019). Why tree lines are lower on islands—Climatic and biogeographic effects hold the
527 answer. *Global Ecology Biogeography*, 28(6), 839-850.
- 528 Ke, G., Meng, Q., Finley, T., Wang, T., Chen, W., Ma, W., Ye, Q., & Liu, T.-Y. (2017).
529 Lightgbm: A highly efficient gradient boosting decision tree. *Advances in Neural*
530 *Information Processing Systems*, 30, 3146-3154.
- 531 Kim, J.W., & Lee, J.S. (2015). Dynamics of alpine treelines: positive feedbacks and global,
532 regional and local controls. *Journal of Ecology and Environment*, 38(1), 1-14.
- 533 Körner, C. & Paulsen, J. (2004). A world-wide study of high altitude treeline temperatures.
534 *Journal of Biogeography*, 31(5), 713-732.
- 535 Körner, C., Jetz, W., Paulsen, J., Payne, D., Rudmann-Maurer, K., & M. Spehn, E. (2017). A
536 global inventory of mountains for bio-geographical applications. *Alpine Botany*, 127(1),
537 1-15.
- 538 Kruse, S., & Herzsuh, U. (2022). Regional opportunities for tundra conservation in the next
539 1000 years. *eLife*, 11, e75163.
- 540 Liang, E., Dawadi, B., Pederson, N., & Eckstein, D. (2014). Is the growth of birch at the upper
541 timberline in the Himalayas limited by moisture or by temperature? *Ecology*, 95(9), 2453-
542 2465.
- 543 Lyu, L., Zhang, Q.B., Pellatt, M.G., Büntgen, U., Li, M.H., & Cherubini, P. (2019). Drought
544 limitation on tree growth at the Northern Hemisphere's highest tree line.
545 *Dendrochronologia*, 53, 40-47.
- 546 Lopatin, E., Kolström, T., & Spiecker, H. (2006). Determination of forest growth trends in
547 Komi Republic (northwestern Russia): combination of tree-ring analysis and remote
548 sensing data. *Boreal Environment Research*, 11, 341-353.
- 549 Lu, X., Liang, E., Wang, Y., Babst, F., & Camarero, J.J. (2021). Mountain treelines climb
550 slowly despite rapid climate warming. *Global Ecology and Biogeography*, 30(1), 305-315.
- 551 Mohapatra, J., Singh, C.P., Tripathi, O.P., & Pandya, H.A. (2019). Remote sensing of alpine
552 treeline ecotone dynamics and phenology in Arunachal Pradesh Himalaya. *International*
553 *Journal of Remote Sensing*, 40(20), 7986-8009.

- 554 Mu, H., Li, X., Wen, Y., Huang, J., Du, P., Su, W., Miao, S., & Geng, M. (2022). A global
555 record of annual terrestrial Human Footprint dataset from 2000 to 2018. *Scientific Data*,
556 9(1), 176.
- 557 Paulsen, J. & Körner, C. (2014) A climate-based model to predict potential treeline position
558 around the globe. *Alpine Botany*, 124(1), 1-12.
- 559 Potapov, P., Turubanova, S., Tyukavina, A., Krylov, A., McCarty, J., Radeloff, V., & Hansen,
560 M. (2015). Eastern Europe's forest cover dynamics from 1985 to 2012 quantified from
561 the full Landsat archive: *Remote Sensing of Environment*, 159, 28-43.
- 562 Piao, S., Ciais, P., Huang, Y., Shen, Z., Peng, S., Li, J., Zhou, L., Liu, H., Ma, Y., Ding, Y. and
563 Friedlingstein, P. (2010). The impacts of climate change on water resources and agriculture
564 in China. *Nature*, 467(7311), 43-51.
- 565 Ren, P., Rossi, S., Camarero, J.J., Ellison, A.M., Liang, E., & Peñuelas, J. (2018). Critical
566 temperature and precipitation thresholds for the onset of xylogenesis of *Juniperus*
567 *przewalskii* in a semi-arid area of the north-eastern Tibetan Plateau. *Annals of Botany*,
568 121(4), 617-624.
- 569 Sigdel, S.R., Wang, Y., Camarero, J.J., Zhu, H., Liang, E., & Peñuelas, J. (2018). Moisture-
570 mediated responsiveness of treeline shifts to global warming in the Himalayas. *Global*
571 *Change Biology*, 24(11), 5549-5559.
- 572 Tachikawa, T., Hato, M., Kaku, M., & Iwasaki, A. (2011). Characteristics of ASTER GDEM
573 version 2. In: 2011 IEEE International Geoscience and Remote Sensing Symposium:
574 IEEE, 3657-3660.
- 575 Tarnocai, C., Canadell, J.G., Schuur, E.A.G., Kuhry, P., Mazhitova, G., & Zimov, S. (2009).
576 Soil organic carbon pools in the northern circumpolar permafrost region. *Global*
577 *Biogeochemical Cycles*, 23, GB2023.
- 578 Testolin, R., Attorre, F., & Jiménez-Alfaro, B. (2020). Global distribution and bioclimatic
579 characterization of alpine biomes. *Ecography*, 43(6), 779-788.
- 580 Verrall, B. & Pickering, C.M. (2020). Alpine vegetation in the context of climate change: A
581 global review of past research and future directions. *Science of the Total Environment*,
582 748, 141344.
- 583 Wang, X., Wang, T., Xu, J., Shen, Z., Yang, Y., Chen, A., Wang, S., Liang, E., & Piao, S.
584 (2022). Enhanced habitat loss of the Himalayan endemic flora driven by warming-forced
585 upslope tree expansion. *Nature Ecology & Evolution*, 6(7), 890-899.
- 586 Wardle, P. & Coleman, M. (1992). Evidence for rising upper limits of four native New Zealand
587 forest trees. *New Zealand Journal of Botany*, 30(3), 303-314.

- 588 Wei, C., Karger, D.N., & Wilson, A.M. Spatial detection of alpine treeline ecotones in the
589 Western United States. *Remote Sensing of Environment*, 2020, 240, 111672.
- 590 Wilmking, M., Harden, J., & Tape, K. (2006). Effect of tree line advance on carbon storage in
591 NW Alaska. *Journal of Geophysical Research*, 111, 1-10.
- 592 Xu, D., Geng, Q., Jin, C., Xu, Z., & Xu, X. (2020). Tree Line Identification and Dynamics under
593 Climate Change in Wuyishan National Park Based on Landsat Images. *Remote Sensing*,
594 12(18), 2890.
- 595

For Review Only

596 **Figure Legends**

597 **Figure 1. Global distribution of closed-loop mountain treeline (CLMT) elevation.** To
598 improve readability, figure **a** is based on the mean value of each closed-loop mountain treeline
599 (at each 30-m pixel). Grey boundaries indicate mountain regions defined by GMBA inventory
600 data. **b–g** show examples of CLMT extraction results superimposed with Google Earth images.
601 The yellow line represents the position of the treeline, and the green circle shows the highest
602 elevation point that formed the starting point of each search by the treeline algorithm.

603

604 **Figure 2. Global latitudinal and longitudinal variation of closed-loop mountain treeline**
605 **(CLMT) elevation.** Different symbols represent different regions and colours represent the
606 distance to the coast. The data points show the mean elevation of all of the pixels in the CLMT.
607 The error bar is the elevation range of the corresponding treeline loop.

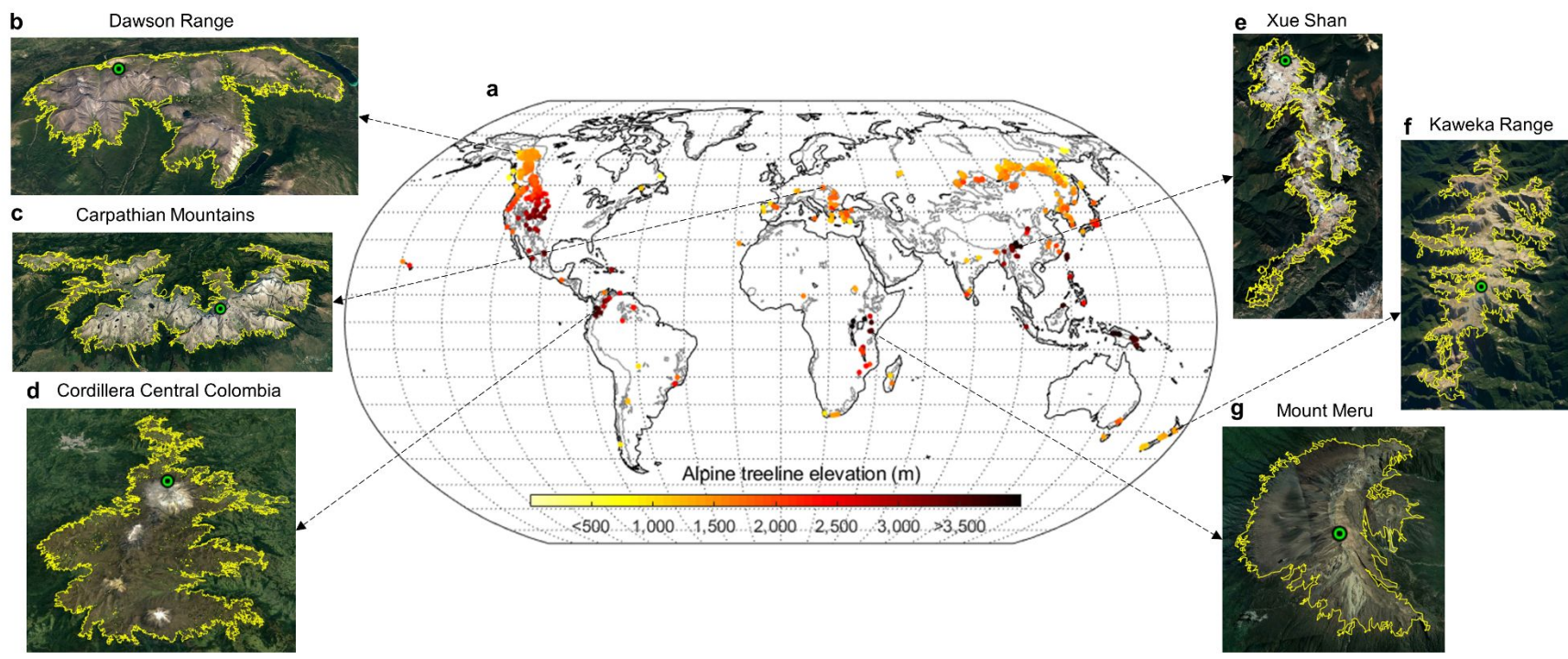
608

609 **Figure 3. Climate drivers controlling the variability in treeline elevation for the globe (a),**
610 **boreal ($\geq 50^\circ\text{N}$, b), temperate ($23.5^\circ - 50^\circ\text{N/S}$, c) and tropical ($23.5^\circ\text{N} - 23.5^\circ\text{S}$, d) regions.**

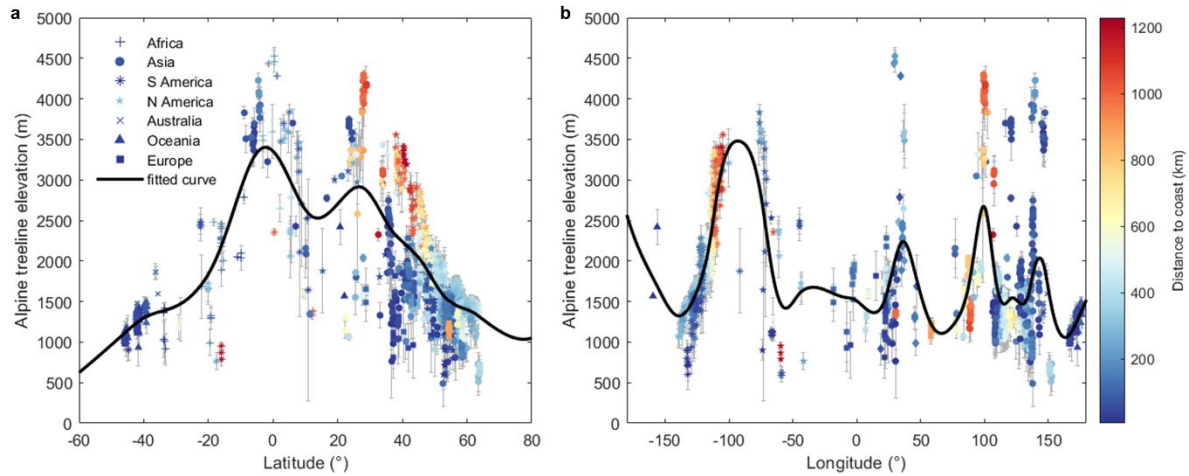
611

612 **Figure 4. Closed-loop mountain treeline (CLMT) shift rate during 2000-2010.** **a**, Spatial
613 pattern of CLMT shift rate. **b**, Box-plot showing CLMT shift rate in boreal ($\geq 50^\circ\text{N}$), temperate
614 ($23.5^\circ - 50^\circ\text{N/S}$) and tropical ($23.5^\circ\text{N} - 23.5^\circ\text{S}$) regions (central line: median; red dot: mean;
615 box: 25th and 75th percentiles, respectively; error bar: maximum and minimum whisker values;
616 +: maximum and minimum values). The black dashed line is the zero line. Numbers of the
617 studied CLMT are shown above the boxes.

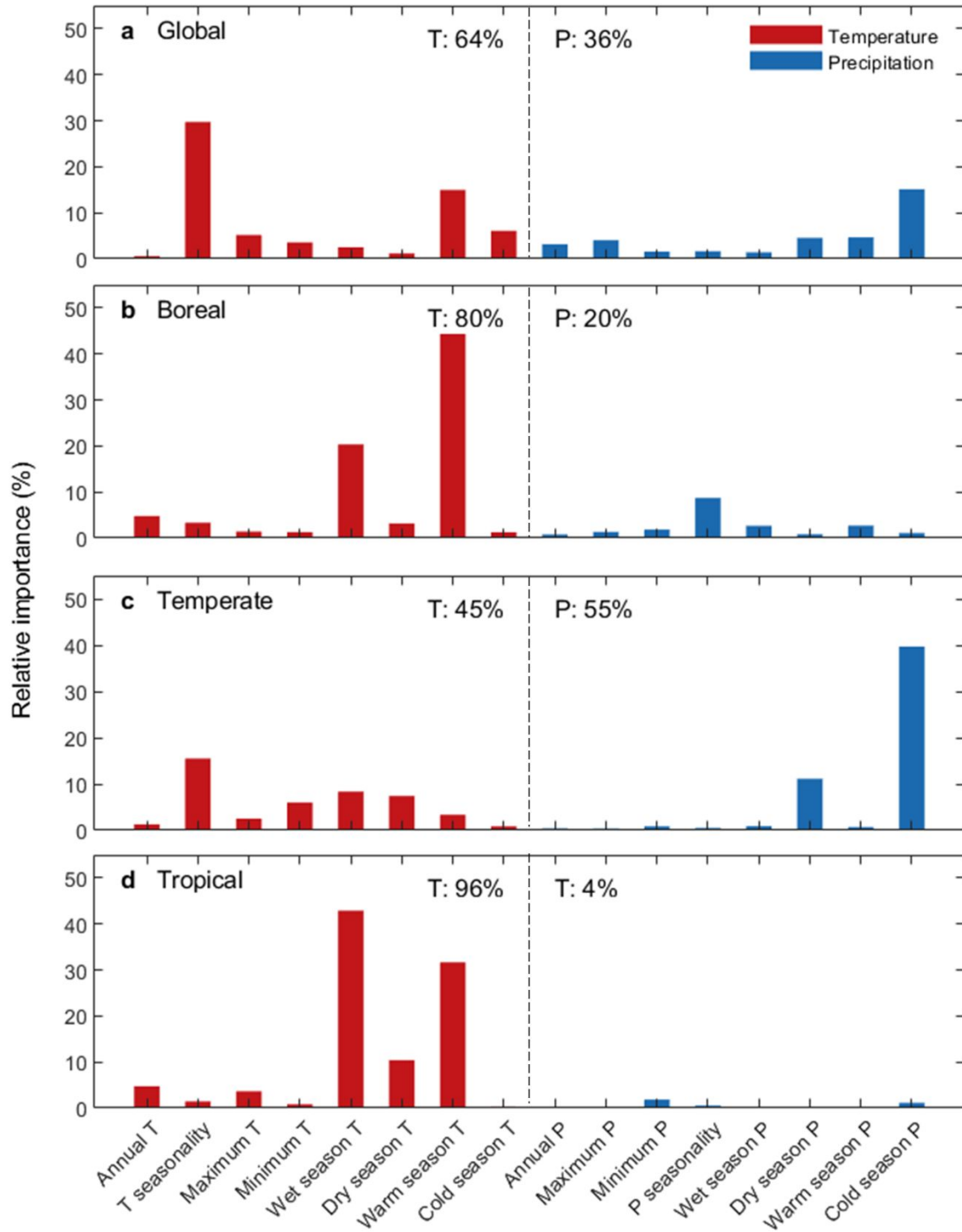
618



619
 620 **Figure 1. Global distribution of closed-loop mountain treeline (CLMT) elevation.** To improve readability, figure a is based on the
 621 mean value of each closed-loop mountain treeline (at each 30-m pixel). Grey boundaries indicate mountain regions defined by GMBA
 622 inventory data. **b–g** show examples of CLMT extraction results superimposed with Google Earth images. The yellow line represents the
 623 position of the treeline, and the green circle shows the highest elevation point that formed the starting point of each search by the treeline
 624 algorithm.
 625

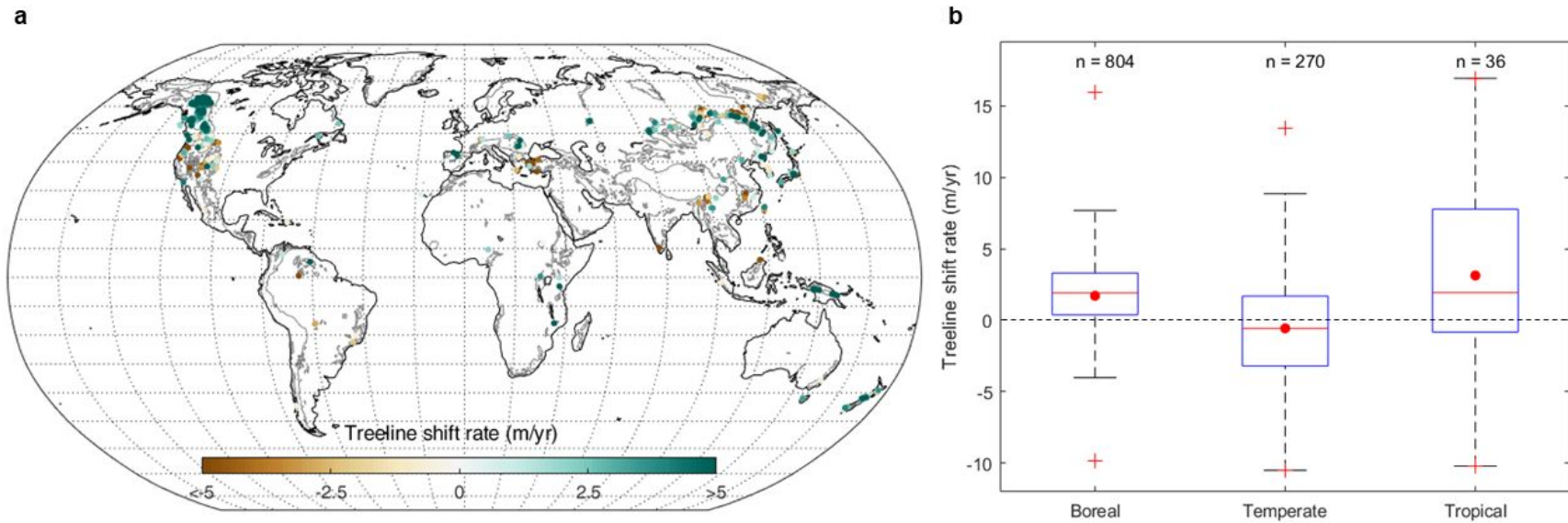


626
627 **Figure 2. Global latitudinal and longitudinal variation of closed-loop mountain treeline**
628 **(CLMT) elevation.** Different symbols represent different regions and colours represent the
629 distance to the coast. The data points show the mean elevation of all of the pixels in the CLMT.
630 The error bar is the elevation range of the corresponding treeline loop.



631
 632 **Figure 3. Climate drivers controlling the variability in treeline elevation for the globe (a),**
 633 **boreal ($\geq 50^\circ\text{N}$, b), temperate ($23.5^\circ - 50^\circ\text{N/S}$, c) and tropical ($23.5^\circ\text{N} - 23.5^\circ\text{S}$, d) regions.**

634



635

636 **Figure 4. Closed-loop mountain treeline (CLMT) shift rate during 2000-2010. a**, Spatial pattern of CLMT shift rate. **b**, Box-plot
 637 showing the CLMT shift rate in boreal ($\geq 50^\circ\text{N}$), temperate ($23.5^\circ - 50^\circ\text{N/S}$) and tropical ($23.5^\circ\text{N} - 23.5^\circ\text{S}$) regions (central line: median;
 638 red dot: mean; box: 25th and 75th percentiles, respectively; error bar: maximum and minimum whisker values; +: maximum and minimum
 639 values). The black dashed line is the zero line. Numbers of the studied CLMT are shown above the boxes.